Clim. Past Discuss., 11, 279–305, 2015
www.clim-past-discuss.net/11/279/2015/
doi:10.5194/cpd-11-279-2015


Climate of the Past Discussions



# Paleoclimate forcing by the solar De Vries/Suess cycle

**H.-J. Lüdecke**[1,*], **C. O. Weiss**[2,*], **and A. Hempelmann**[3]

[1]HTW, University of Applied Sciences, Saarbrücken, Germany
[2]Physikalisch-Technische Bundesanstalt, Braunschweig, Germany
[3]University of Hamburg, Hamburg Observatory, Hamburg, Germany
[*]retired

Received: 8 December 2014 – Accepted: 21 January 2015 – Published: 12 February 2015

Correspondence to: H.-J. Lüdecke (moluedecke@t-online.de)

Published by Copernicus Publications on behalf of the European Geosciences Union.



## Abstract

A large number of investigations of paleoclimate have noted the influence of a ∼200 year oscillation which has been related to the De Vries/Suess cycle of solar activity. As such studies were concerned mostly with local climate, we have used extensive northern hemispheric proxy data sets of Büntgen and of Christiansen/Ljungqvist together with a southern hemispheric tree-ring set, all with 1 year time resolution, to analyze the climate influence of the solar cycle. As there is increasing interest in temperature rise rates, as opposed to present absolute temperatures, we have analyzed temperature differences over 100 years to shed light on climate dynamics of at least the last 2500 years. Fourier- and Wavelet transforms as well as nonlinear optimization to sine functions show the dominance of the ∼200 year cycle. The sine wave character of the climate oscillations permits an approximate prediction of the near future climate.

## 1 Introduction

The search for cycles on nearly all time scales in time series of temperatures, precipitations and droughts has a long tradition. The physical mechanisms of these cycles are mostly unknown. As hypotheses, solar modes, auto climate modes (episodic outbursts of big meltwater reservoirs, thermohaline circulation through a threshold response etc.), and cosmic modes governed by big planets are discussed, (Friis-Christensen and Lassen, 1991; Van Geel et al., 2003; Braun et al., 2005; Lohmann and Schöne, 2013; Scafetta, 2012). In the present study we look for dominant climate cycles in the period regime of ∼200 years and their influence on the recent and near future climate. We found no work on auto oscillations in this period range, by contrast, in all papers solar forcing is considered as the main cycle driver.

The studies begin with De Vries (1958) and Suess (1980) who found variations in the production rates of the cosmic isotopes $^{14}C$ and $^{10}Be$. Breitenmoser et al. (2012)

analyze terrestrial temperature proxies and the De Vries/Suess solar activity and find a good correlation, particularly when incorporating volcanic activity. Cliver et al. (1998) show a precise linear dependence of solar magnetic field (thus solar activity) and Earth temperature and estimate the influence of the Sun on the 20th century Earth climate change up to 100 %. Raspopov et al. (2008) find a clear ∼ 200 year cycle and relate it with the solar De Vries/Suess cycle. How closely the Earth temperature is related with the solar De Vries/Suess cycle becomes apparent in the study of Knudsen et al. (2011) who find the characteristic "burst" pattern (1000 years of oscillation, repeating every 2500 years) mirrored in the temperatures derived from stalagmites in subtropical caves of China, Turkey, USA. Novello et al. (2012) find the AMO plus De Vries/Suess cycle the dominant contribution to the nordeast Brazilian climate for the last 3000 years, in correspondence with our results (Lüdecke, 2012). Wagner et al. (2001) demonstrate that the De Vries/Suess cycle of ∼ 205 years is present in $^{10}$Be data from the GRIP ice core during the last ice age, 20 to 50 kyr BP. Liu et al. (2011) find cycles of 1324, 800, 199, and 110 years in tree-rings of the Tibetan Plateau for the past 2485 years and make a prediction that the temperatures will decrease in the future until ∼ AD 2070 and then increase again. Steinhilber and Beer (2013) find in their analysis of solar isotope data the De Vries/Suess cycle as the strongest spectral component and, additionally, give a prediction of future climate for the next 500 years with cooling until ∼ AD 2080. Kern et al. (2012) find the influences of 80, 120, 208, 500, 1000 and 1500 year cycles and show that the De Vries/Suess cycle was a dominant factor for the Earth climate. Zhao and Feng (2015) find periodicities of 208, 521, and ∼ 1000 years in antarctic ice-core records. Evidences of the dominance of the De Vries/Suess cycle of solar activity on terrestrial climate are given in Seidenglanz et al. (2012); Leal-Silva and Herrera (2012); Costas et al. (2012), and Scafetta (2012) to mention just a few of a long list of papers showing the action of the solar De Vries/Suess cycle on the Earth climate. A possible mechanism of solar modulated cosmic rays on cloud cover and thus on Earth climate is investigated in Svensmark (1998); Marsh and Svensmark (2000); Svensmark et al. (2009); Enghoff et al. (2011). An extensive



survey of papers investigating the influence of the Sun on terrestrial climate cycles is given in Lüning (2014). Dima and Lohmann (2008) and Huybers and Wunsch (2003) discuss a rectification hypothesis based on nonlinearity of the terrestrial system. In view of these various investigations of the influence of solar activity on local climate the question of the effects on the global scale arises.

## 2 Differences vs. absolute temperatures

There is interest in temperature rise rates besides the absolute temperatures, for instance applied in trend analysis (Lennartz and Bunde, 2011) or to detect Dansgaard–Oeschger events (Rahmstorf, 2003). Therefore, we looked in yearly records of 100 year temperature differences for cycles. For this purpose, from a yearly temperature time series $T(t_1),\ldots,T(t_L)$ of the $L$ years $t_1,\ldots,t_L$ the pertinent $\Delta T(t)$ record of length $L-100$ is derived as follows: $\Delta T(t_j)$ is the backward temperature difference over 100 years by linear regression $R$,

$$R[T(t_{j-99}),\ldots,T(t_j)] = a_j \cdot t + c_j \tag{1}$$

which yields

$$\Delta T(t_j) = a_j \cdot (t_j - t_{j-99}) \tag{2}$$

Note that the $\Delta T(t)$ record is 100 years shorter than the $T(t)$ record because the first $\Delta T(t)$ value belongs to $t_{100}$.

Differences by linear regression $\Delta T(t)$ are better suited to reveal temperature periodicities in a certain frequency range than temperatures $T(t)$ themselves, because frequency components outside the range are weakened, the differencing acting as a spectral filter. The Fourier spectra of the $T(t)$ and the $\Delta T(t)$ records show the same frequencies but different peak powers. This is plausible since the derivative of a sine function has the same spectrum as the sine function itself, and the $\Delta T(t)$ data are rather similar to a sine function.

## 3 The data

For sufficient resolution in the Fourier analysis and to avoid possible distortions by interpolations, $T(t)$ records of 1 year time resolution are desirable. A length of at least ~ 2000 years is further desirable to avoid Fourier artifacts within the multi centennial region of interest. Recently two appropriate Northern Hemisphere temperature proxy stacks are available extending back to a maximum of −2500 yr BP. One stack (0 to AD 1973) contains 91 temperature proxy series evaluated from tree rings, stalagmites, ice cores, sediments etc. (Christiansen and Ljungqvist, 2012). The other (−499 BP to AD 1993) was evaluated from 7284 tree ring samples, a total of 1546 ring width series, from high elevation conifers from the Austrian Alps (Büntgen et al., 2011). For the Southern Hemisphere a Tasmanian tree ring record of 3592 years exists (Cook et al., 2000). Figure 1 shows the geographic locations of the proxies used in this study. Apart from these records no other publicly available data meet the requirements for the analysis. For a relation with solar activity, we analyzed the production rate record $P(t)$ of the solar isotope abundances of $^{10}$Be and $^{14}$C (Steinhilber et al., 2012), which has a time resolution of 22 years. This $P(t)$ series extends back to −7404 BP. Fourier- and wavelet analyses were given (Steinhilber et al., 2012). Table 1 gives the main characteristics of the records used. Figure 2 shows the data together with their $\Delta T(t)$ resp. $\Delta P(t)$ graphs, constructed according to Eqs. (1) and (2). Since the $P(t)$ record has 22 year time steps we have used 110 years instead of 100 years for the differences.

## 4 Spectral analysis

For the discrete Fourier transform (DFT) the records were padded with 25 000 zeros, yielding optimum interpolation of the DFT spectra. The data were converted to anomalies around the mean and normalized to the SD. The confidence curves with respect to background noise were generated by MC-simulation for which 10 000 random time series are applied with the same lengths and Hurst exponents H as the



pertinent records, in the form of anomalies and normalized to the SD. H was obtained by detrended fluctuation analysis (DFA) (Kantelhardt et al., 2001; Kantelhardt, 2004). With MC-simulation the calculation of the confidence curves is not restricted to red AR1 noise.

Table 2 gives the record lengths, record resolutions, Hurst exponents, DFT periods for the strongest peak in the ~ 200 year period band, and confidence levels. Figure 3 shows the DFT spectra. The ~ 200 year peaks in the NH series Bü and Chr/Lju, as well as the pertinent peak in the Stei/Beer isotope record have powers giving 99 % confidence level against noise, in the SH series of Cook only 95 %.

We note that the spectrum of the $P(t)$ record shows 3 distinct peaks at ~ 200 years. It would seem that this reflects the amplitude modulation AM of the De Vries oscillation (Knudsen et al., 2011) known as the “Suess bursts” (1000 years of strong oscillation amplitude followed by weaker oscillation, repeating every 2500 years. Spectrum of an AM being a central carrier with two sidebands).

Figure 4 shows the wavelet analysis (Torrence and Compo, 1998) of the $T(t)$ resp. $P(t)$ records, Fig. 6 the cross wavelets (Grinsted et al., 2004). Because the Stei/Beer record with 22 year steps and its 1 year step interpolated version show no difference in DFT, the interpolated version was applied for the wavelet analysis. All wavelet spectra exhibit variations in power and frequency over the time. We mention that the NH records Bü and Chr/Lju have a disruption of the cycle regularity around the years ~ AD 700 whereas in the SH (Cook) similar disruptions are centered around ~ AD 500 and ~ AD 1500. Contrasting to the NH records, the periodicity of the Cook record is weak for the years > AD 1400.

## 5 Sine wave fit by nonlinear optimization

The appearance of Fig. 2 suggests that the $\Delta T(t)$ and $\Delta P(t)$ records can be reasonably represented by single sine functions

$$\Delta T_{\mathrm{sin}e} \text{ (resp. } \Delta P_{\mathrm{sin}e}) = \sin(2\pi\nu \cdot t + \varphi) \tag{3}$$

The parameters of the sine function $\nu$ and $\varphi$ could in principle be taken from the DFT. However, DFT has uncertainty margins and treats the data as infinite recurrences, which is equivalent to compulsory boundary conditions

$$\sin(2\pi\nu \cdot t_{\mathrm{start}} + \varphi) = \sin(2\pi\nu \cdot t_{\mathrm{end}} + \varphi) \tag{4}$$

To avoid this restrictions and associated possible artifacts, the frequency $\nu$ and the phases $\varphi$ of the sine representations $\Delta T_{\mathrm{sine}}$ and $\Delta P_{\mathrm{sine}}$ were determined by nonlinear optimization (Nelder and Mead, 1965). The objective function $F(\nu, \varphi)$ to be minimized is the negative Pearson correlation between $X = \Delta T_{\mathrm{sine}}$ and $Y = \Delta T(t)$ resp. $X = \Delta P_{\mathrm{sine}}$ and $Y = \Delta P(t)$

$$F(\nu, \varphi) = -\rho_{\mathrm{XY}} = -\frac{\mathrm{cov}(X, Y)}{\sigma_X \sigma_Y} \tag{5}$$

As the result, we find nearly the same frequencies for all records as in DFT (see Table 2). Table 3 shows parameters and results of the nonlinear optimization. Figure 6 shows the difference records $\Delta T(t)$ and $\Delta P(t)$ together with the pertinent sine representations. The running correlations for a 200 year window are given in Fig. 7, showing a notable common gap of correlation around ~ AD 700 for the Bü and Chr/Lju series. The disruption of the climate cycle which occurs for the two NH temperature stacks Bü and Chr/Lju around ~ AD 700 (see Fig. 6) is visible also in the wavelets (see Fig. 4) and in the cross wavelets (see Fig. 5, left middle, right upper, and right middle panel). The corresponding is valid for the SH Cook series at ~ 500 and ~ AD 1500. In these perturbation zones the phases appear to be reversing.



We note that the 20th century $\Delta T(t)$ maximum is comparable in magnitude with the past maxima. Thus, the proxies used in this paper show that the warming rate during the 20th century lies within the natural rates of change.

The correlation of the $\Delta T(t)$ records Bü and Chr/Lju (AD 99–1973) is 0.45. The higher correlation of these records with sine functions $\Delta T_{\mathrm{sine}}$ indicates that the essential content of the two records is their periodic character.

The sine representation over the 9307 years of the Stei/Beer difference record yields a correlation of only 0.21, apparently due to phase noise during the long time. For a test, we divided the record into subsections of ~ 2330 years and find higher correlations with periods and phases given in the rows 4.0–4.3 of Table 3. According to this, the ~ 200 year cycle varies between 185 and 230 years in period length. In a corresponding wavelet diagram (Knudsen et al., 2011) the period is found to shift up to ~ 240 years in 5000 yr BP, in agreement with our finding given in Table 3 and in the left upper panel of Fig. 4.

## 6 Phase noise of the climate cycle

To identify reasonably maxima and minima in Fig. 6 as real extrema, we must define an objective criterion. Since each record is represented by a single sine function, we define the following criterion for a cycle maximum: it must lie within less than half of the sine period to a sine maximum and exceed 1/2 of the data SD. If more than one maximum satisfies this condition, we choose the strongest one. Admissible maxima which only fail the "standard-deviation-condition" are still counted if the Pearson correlation of the data with the sine representation exceeds 0.4 during the time interval between two neighboring sine minima. The corresponding criterion applies with the minima. Figure 8 shows the time deviations of the maxima and minima from the sine wave extrema (Fig. 6) demonstrating a good cycle stability over the whole duration of ~ 2500 years.

## 7 Confidence levels

In order to ascertain a statistical confidence level of the correlation between the data and the sine-representations (see Fig. 6), we assumed the Null hypothesis that the correlation is caused by chance. We tested the Null hypothesis by Monte Carlo simulations, in each case with 10 000 random surrogate records of the same length and the same Hurst exponent H as the pertinent time series $T(t)$ resp. $P(t)$ given in Table 2. The surrogate time series were converted into difference records $\Delta T(t)$ resp. $\Delta P(t)$ according to Eqs. (1) and (2). Next, the Pearson correlations of these surrogates with the pertinent sine representations $\Delta T_{\text{sine}}$ resp. $\Delta P_{\text{sine}}$ given in Table 3 were calculated. The following numbers of surrogates out of 10 000 had better or equal correlations with the pertinent sines: 6 for Bü, 3 for Chr/Lju, 42 for Cook, and 0 for Stei/Beer. As a consequence, the Null hypothesis can be rejected with a confidence level of 99.9 % for Chr/Lju, Bü, and Stei/Beer and of 95 % for Cook.

Besides 100 year linear regression length, we tested also the lengths 50 and 150 years for all temperature records. However, the sine representation by nonlinear optimization becomes more difficult for the 50 year length because the algorithm tends to be trapped in local minima. With 50 year length, the values of the correlations for all records are distinctly worse than for 100 year length. With 150 year length, again neither significant differences to 100 year length in the optimum period arise, however, the correlations with the pertinent sine representations become somewhat better. In order to verify that in the period-phase plane no better correlations than those with the sine representations cited in Table 3 exist, we optimized the difference records through all sine periods from 50 years until 200 years in 0.1 year steps evaluating in every step only the sine phases by nonlinear optimization. As a result, no better correlations than those belonging to the "De Vries/Suess" periods, cited in Table 3, are found. Thus, choice of a 100 year linear regression length appears not to cause systematics.



## 8 Tentative prediction of the climate future

The Earth's climate shows a rather regular oscillation of ∼ 200 year period during the last millennia. However, frequency, phase, and strength of the oscillation are found to vary in different time series of temperatures and for different times (see Figs. 4–6, and 8). Nonetheless, the relative historic stability of the cycle suggests that the periodic nature of the climate will persist also for the foreseeable future. Disregarding other conceivable forcings e.g. anthropogenic influences, an approximate prediction of the climate for the next 100 years suggests itself. Figure 9 shows the $T_{\text{sine}}$ representation from AD 1800 to AD 2100 derived from the $\Delta T_{\text{sine}}$ representation by a $\pi/2$ phase shift. It gives correctly the 1850–1900 temperature minimum and shows a temperature drop from present to ∼ AD 2080, the latter comparable with the minimum of 1870, as already predicted in the studies (Steinhilber and Beer, 2013; Liu et al., 2011) on the grounds of solar activity data alone.

## 9 Summary and discussion

We have analyzed the differences of temperatures resp. isotope production rates of the most extensive paleoclimate temperature proxy sets for the NH and the SH (Christiansen and Ljungqvist, 2012; Büntgen et al., 2011; Cook et al., 2000) and an isotopes production time series (Steinhilber and Beer, 2013). The methods are spectral, including wavelet analyses and nonlinear optimization fitting of single sine functions to the records. The global picture emerges of a ∼ 200 year period climate oscillation which correlates highly with the De Vries/Suess oscillation of solar activity. This would indicate that the dominant forcing of the paleoclimate is the solar activity.

For different records and different times, however, we find frequencies differing slightly from the main ∼ 200 year periodicity. The solar influence is modified by the response of the Earth system and its inherent forcings such as volcanic activity. Such a response can cause time delays to which the phase delays between the climate time-

series $\Delta T(t)$ may be attributed. The terrestrial activities may dominate the solar activity temporarily, e.g. disrupting the sine-like oscillations. Such disruptions are clearly visible in Figs. 4–7. They can affect the oscillation amplitude as well as the phase. For longer term changes in phase and amplitude one may keep in mind a modulation of the higher frequency oscillations (e.g. the ∼200 year period De Vries/Suess cycle) by lower frequency –, i. e. millennial period cycles. Zhao and Feng (2015) showed that the millennial cycles exhibit high phase stability compared to the centennial cycles. This could show such a modulation, which is by all means to be expected in view of the nonlinearities of the terrestrial system, and even for the sun system itself, as the different frequencies in the rows 4.0–4.4 of Table 3 show. By such modulation, continuous phase changes over a long time can occur, equivalent to frequency shifts as mentioned above, such as we and also Zhao/Feng find them in different proxies and for different times. We observe that the unequal strength of the sidebands of the ∼ 200 year period oscillation of the solar activity (Fig. 3 left upper panel) is consistent with a simultaneous modulation of amplitude and phase. Evidently with the proxies available of only 10 to 12 De Vries/Suess cycles such cross modulation between cycles cannot be unambiguously proven, but nonetheless is a possible explanation for the differing frequencies.

*Acknowledgements.* We thank Sebastian Lüning for helpful discussions and providing us with additional references to the interdependence of solar activity and climate change.

## References

Braun, H., Christl, M., Rahmstorf, S., Ganopolski, A., Mangini, A., Kubatzki, C., Roth, K., and Kromer, B.: Possible solar origin of the 1,470-year glacial climate cycle demonstrated in a coupled model, Nature, 438, 208–211, 2005. 280

Breitenmoser, P., Beer, J., Brönnimann, S., Frank, D., Steinhilber, F., and Wanner, H.: Solar and volcanic fingerprints in tree-ring chronologies over the past 2000 years, Palaeogeogr. Palaeocl., 313–314, 127–139, 2012. 280



Büntgen, U., Tegel, W., Nicolussi, K., McCormick, M., Frank, D., Trouet, V., Kaplan, J. O., Herzig, F., Heussner, K.-U., Wanner, H., Luterbacher, J., and Esper, J.: 2500 years of European climate variability and human susceptibility, Science, 331, 578–582, doi:10.1126/science.1197175, 2011. 283, 288, 294, 297, 298, 299, 300

Christiansen, B. and Ljungqvist, F. C.: The extra-tropical Northern Hemisphere temperature in the last two millennia: reconstructions of low-frequency variability, Clim. Past, 8, 765–786, doi:10.5194/cp-8-765-2012, 2012. 283, 288, 294, 297, 298, 299, 300

Cliver, E. W., Boriakoff, V., and Feynman, J.: Solar variability and climate change: geomagnetic aa index and global surface temperature, Geophys. Res. Lett., 25, 1035–1038, 1998. 281

Cook, E. R., Buckley, B. M., D'Arrigo, R. D., and Peterson, M. J.: Warm-season temperatures since 1600 BC reconstructed from Tasmanian tree rings and their relationship to large-scale sea surface temperature anomalies, Clim. Dynam., 16, 79–91, 2000. 283, 288, 294, 297, 298, 299, 300

Costas, S., Jerez, S., Trigo, R. M., Goble, R., and Rebelo, L.: Sand invasion along the Portuguese coast forced by westerly shifts during cold climate events, Quaternary Sci. Rev., 42, 15–28, 2012. 281

De Vries, H.: Variation in concentration of radiocarbon with time and location on Earth, K. Ned. Akad. Van. Wet.-B, 61, 94–102, 1958. 280

Dima, M. and Lohmann, G.: Conceptual model for millenial climate variability: a possible combined solar-thermohaline circulation origin for the ∼ 1,500-year cycle, Clim. Dynam., 32, 301–311, 2008. 282

Enghoff, M. B., Pedersen, J. O. P., Uggerhoj, U. I., and Paling, S. M.: Aerosol nucleation induced by a high energy particle beam, Geophys. Res. Lett., 38, L09805, doi:10.1029/2011GL047036, 2011. 281

Friis-Christensen, E. and Lassen, K.: Length of the solar cycle: an indicator of solar activity closely associated with climate, Science, 254, 698–700, 1991. 280

Grinsted, A., Moore, J. C., and Jevrejeva, S.: Application of the cross wavelet transform and wavelet coherence to geophysical time series, Nonlin. Processes Geophys., 11, 561–566, doi:10.5194/npg-11-561-2004, software available at: http://noc.ac.uk/using-science/crosswavelet-wavelet-coherence (last access: February 2015), 2014. 284, 301

Huybers, P. and Wunsch, C.: Rectification and precession signals in the climate system, Geophys. Res. Lett., 30, 2011, doi:10.1029/2003GL017875, 2003. 282

Kantelhardt, J. W.: Fluktuationen in komplexen Systemen, Habilitationsschrift, Universität Gießen, Germany, available at: http://www.physik.uni-halle.de/Fachgruppen/kantel/habil.pdf (last access: February 2015), 2004. 284

Kantelhardt, J. W., Koscielny-Bunde, E., Rego, H. H. A., Havlin, S., and Bunde, A.: Detecting long-range correlations with detrended fluctuation analysis, Physica A, 295, 441–454, 2001. 284

Kern, A. K., Harzhauser, M., Piller, W. E., Mandic, O., and Soliman, A.: Strong evidence for the influence of solar cycles on a Late Miocene lake system revealed by biotic and abiotic proxies, Palaeogeogr. Palaeocl., 329–330, 124–136, 2012. 281

Knudsen, M. F., Jacobsen, B. H., Riisager, P., Olsen, J., and Seidenkrantz, M.-S.: Evidence of Suess solar-cycle bursts in subtropical Holocene speleothem $\delta^{18}$O records, Holocene, 22, 597–602, 2011. 281, 284, 286

Leal-Silva, M. C. and Velasco Herrera, V. M.: Solar forcing on the ice winter severity index in the western Baltic region, J. Atmos. Sol-Terr. Phy., 89, 98–109, 2012. 281

Lennartz, S. and Bunde, A.: Distribution of natural trends in long-term correlated records: a scaling approach, Phys. Rev. E, 84, 021129, doi:10.1103/PhysRevE.84.021129, 2011. 282

Liu, Y., Cai, Q., Song, H., An, Z., and Linderholm, H. W.: Amplitudes, rates, periodicities and causes of temperature variations in the past 2485 years and future trends over the central-eastern Tibetan Plateau, Chinese Sci. Bull., 56, 2986–2994, doi:10.1007/s11434-011-4713-7, 2011. 281, 288

Lohmann, G. and Schöne, B. R.: Climate signatures on decadal to interdecadal time scales as obtained from mollusk shells (Arctica islandica) from Iceland, Palaeogeogr. Palaeocl., 373, 152–162, 2013. 280

Lüdecke, H.-J., Hempelmann, A., and Weiss, C. O.: Multi-periodic climate dynamics: spectral analysis of long-term instrumental and proxy temperature records, Clim. Past, 9, 447–452, doi:10.5194/cp-9-447-2013, 2013. 281

Lüning, S.: Compilation of references of solar-climate cycles, available at: www.klimaargumente.de/#sonne (last access: February 2015), and chrono.qub.ac.uk/blaauw/cds.html (last access: February 2015), 2014. 282

Marsh, N. and Svensmark, H.: Low cloud properties influenced by cosmic rays, Phys. Rev. Lett., 85, 5004–5007, 2000. 281

Nelder, J. A. and Mead, R.: A simplex method for function minimization, Comput. J., 7, 308–313, doi:10.1093/comjnl/7.4.308, 1965. 285



Novello, V. F., Cruz, F. W., Karmann, I., Burns, S. J., Strikis, N. M., Vuille, M., Cheng, H., Edwards, R. L., Santos, R. V., Frigo, E., and Barreto, E. A. S.: Multidecadal climate variability in Brazil's Nordeste during the last 3000 years based on speleothem isotope records, Geophys. Res. Lett., 39, L23706, doi:10.1029/2012GL053936, 2012. 281

Rahmstorf, S.: Timing of abrupt climate change: a precise clock, Geophys. Res. Lett., 30, 1510, doi:10.1029/2003GL017115, 2003. 282

Raspopov, O. M., Dergachev, V. R., Esper, J., Kozyreva, O. V., Frank, D., Ogurtsov, M., Kolström, T., and Shao, X.: The influence of the de Vries (~200-year) solar cycle on climate variations: results from the Central Asian Mountains and their global link, Palaeogeogr. Palaeocl., 259, 6–16, 2008. 281

Scafetta, N.: Multi-scale harmonic model for solar and climate cyclical variation throughout the Holcene based on Jupiter-Saturn tidal frequencies plus the 11-year solar dynamo cycle, J. Atmos. Sol-Terr. Phy., 80, 296–311, 2012. 280, 281

Seidenglanz, A., Prange, M., Varma, V., and Schulz, M.: Ocean temperature response to idealized Gleissberg and de Vries solar cycles in a comprehensive climate model, Geophys. Res. Lett., 39, L22602, doi:10.1029/2012GL053624, 2012. 281

Steinhilber, F. and Beer, J.: Prediction of solar activity for the next 500 years, J. Geophys. Res.-Space, 118, 1861–1867, 2013. 281, 288, 294, 298, 299, 300

Steinhilber, F., Abreu, J. A., Beer, J., Brunner, I., Christl, M., Fischer, H., Heikkilä, U., Kubik, P. W., Mann, M., McCracken, K. G., Miller, H., Miyahara, H., Oerter, H., and Wilhelms, F.: 9,400 years of cosmic radiation and solar activity from ice cores and tree rings, P. Natl. Acad. Sci. USA, 109, 5967–5971, doi:10.1073/pnas.1118965109, 2012. 283

Suess, H. E.: The radiocarbon record in tree rings of the last 8000 years, Radiocarbon, 22, 200–209, 1980. 280

Svensmark, H.: Influence of cosmic rays on Earth's climate, Phys. Rev. Lett., 81, 5027–5030, 1998 281

Svensmark, H., Bondo, T., and Svensmark, J.: Cosmic ray decreases affect atmospheric aerosols and clouds, Geophys. Res. Lett., 36, L15101, doi:10.1029/2009GL038429, 2009. 281

Torrence, C. and Compo, P.: A practical guide to wavelet analysis, Bulletin of the AMS, 79, 61–78, 1998. 284

Van Geel, B., van der Plicht, J., and Renssen, H.: Major $\Delta^{14}C$ excursions during the late glacial and early Holocene: changes in ocean ventilation or solar forcing of climate change?, Quatern. Int., 105, 71–76, 2003. 280

Wagner, G., Beer, J., Masarik, J., Muscheler, R., Mende, W., Kubik, P. W., Laj, C., Raisbeck, G. M., and Yiou, F.: Presence of the solar De Vries cycle (~ 205 years) during the last ice age, Geophys. Res. Lett., 28, 303–306, 2001. 281

Zhao, X. H. and Feng, X. S.: Correlation between solar activity and the local temperature of Antarctica during the past 11,000 years, J. Atmos. Sol.-Terr. Phys. 122, 26–33, 2015. 281, 289



**Table 1.** Characteristics of the records used: Bü (Büntgen et al., 2011), Chr/Lju (Christiansen and Ljungqvist, 2012), Cook (Cook et al., 2000), and Stei/Beer (Steinhilber and Beer, 2013).

| Record | Data | Method | Season | Resolution [years] | Time span BC/AD |
|---|---|---|---|---|---|
| Bü | proxy-temperatures | tree rings | summer | 1 | −499 until 2003 |
| Chr/Lju | proxy-temperatures | multi | all | 1 | 0 until 1973 |
| Cook | proxy-temperatures | tree rings | summer | 1 | −1600 until 1991 |
| Stei/Beer | isotopes production rates | $^{10}Be$, $^{14}C$ | all | 22 | −7404 until 2012 |

**Table 2.** Parameters and results of DFT.

| $T(t)$ resp. $P(t)$ record | Length [years] | Resolution [years] | Hurst exponent | ~ 200 year peak period [years] | Peak confidence level [%] |
|---|---|---|---|---|---|
| Bü | 2503 | 1 | 1 | 186.0 | 99 |
| Chr/Lju | 1974 | 1 | 1.1 | 189.4 | 99 |
| Cook | 3592 | 1 | 0.9 | 200.8 | 95 |
| Stei/Beer | 9417 | 22 | 0.6 | 202.2 | > 99 |





**Table 3.** Single sine representations of the difference records $\Delta T(t)$ resp. $\Delta P(t)$ by nonlinear optimization (phases given in radians). The piecewise optimizations for the Steinhilber/Beer data (No. 4.1–4.3) and the total length optimizations for the records Stei/Beer (No. 4.4 compared with No. 4.0) and Cook (No. 3.0 compared with No. 3.1) demonstrate the variations of periods and phases over the time. We mention that the $\Delta T(t)$ resp. $\Delta P(t)$ records start 100 resp. 110 years later than the $T(t)$ resp. $P(t)$ records (see Table 1).

| No. | Record | from | to | duration | sine period | sine phase | cor |
|---|---|---|---|---|---|---|---|
| | | [BC/AD] | | [years] | | | |
| 1.0 | Bü | −400 | 2003 | 2404 | 184.0 | 4.483 | 0.49 |
| 2.0 | Chr/Lju | 99 | 1973 | 1875 | 189.9 | 0.046 | 0.58 |
| 3.0 | Cook | −401 | 1991 | 2393 | 199.7 | 2.481 | 0.41 |
| 3.1 | Cook | −1501 | 1991 | 3493 | 204.8 | 3.056 | 0.36 |
| 4.0 | Stei/Beer | −408 | 2012 | 2421 | 203.0 | 1.775 | 0.68 |
| 4.1 | Stei/Beer | −7294 | −4962 | 2332 | 228.1 | 3.788 | 0.47 |
| 4.2 | Stei/Beer | −4962 | −2630 | 2332 | 230.9 | 6.202 | 0.34 |
| 4.3 | Stei/Beer | −2630 | −320 | 2310 | 215.5 | 0.919 | 0.45 |
| 4.4 | Stei/Beer | −7294 | 2012 | 9417 | 232.1 | 0.236 | 0.21 |

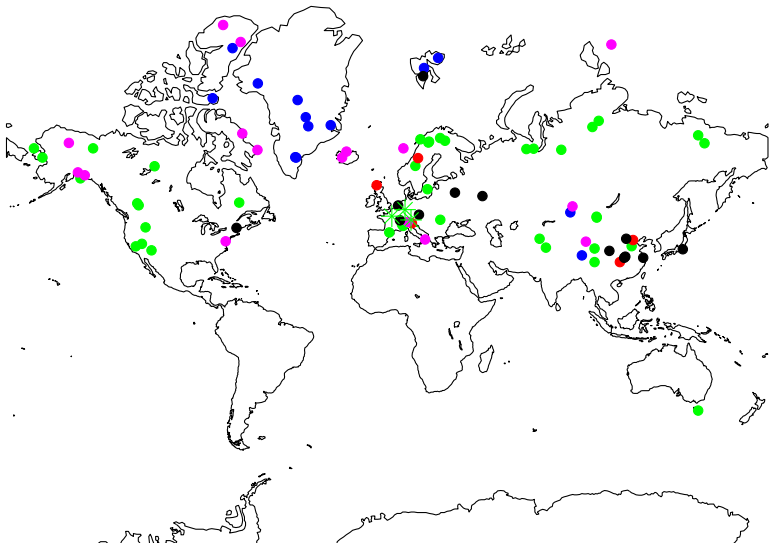

**Figure 1.** (Color online) Global overview of the temperature proxies used in this study. Green color: tree-rings, red color: speleothems, blue color: ice-cores, magenta color: sediments, black color: other as pollen, multi-proxy, documentary, and ice melt layers. 91 sites (Christiansen and Ljungqvist, 2012 and Cook et al., 2000) are depicted, the several thousand tree-ring sites of Büntgen et al. (2011), concentrated in central Europe, are represented by green crosses.





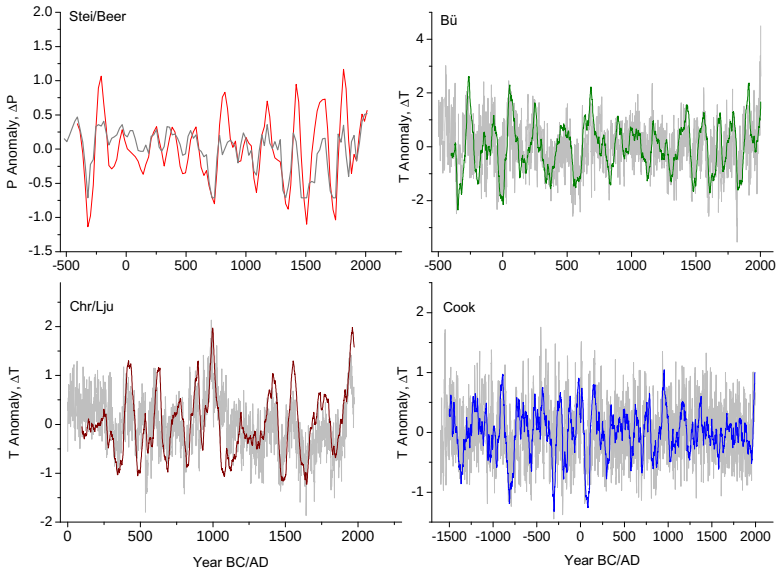


**Figure 2.** (Color online) Proxy temperatures $T(t)$ and cosmic isotopes rate $P(t)$ (grey). Differences $\Delta T(t)$ ($\Delta t$ = 100 years) and $\Delta P(t)$ ($\Delta t$ = 110 years) by linear regression (Eqs. 1 and 2) (blue color). Left upper panel: $P(t)$ and $\Delta P(t)$ (Steinhilber and Beer, 2013) with a linear regression length of 110 years enforced by the 22 year steps of the original $P(t)$ record. Left lower panel: northern hemispheric T(t) and $\Delta T(t)$ from stalagmites, tree rings, sediments, ice cores, pollen etc. (Christiansen and Ljungqvist, 2012). Right upper panel: northern hemispheric $T(t)$ and $\Delta T(t)$ from tree rings (Büntgen et al., 2011). Right lower panel: southern hemispheric $T(t)$ and $\Delta T(t)$ from tree rings (Cook et al., 2000).

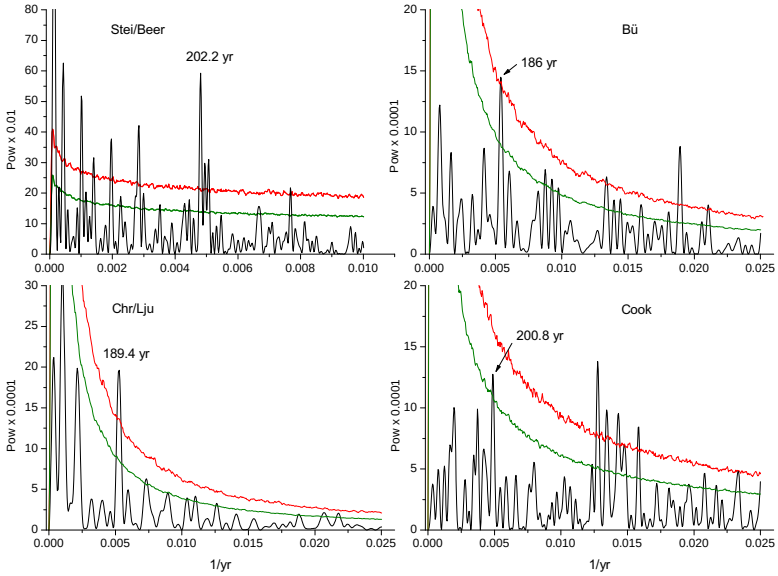


**Figure 3.** (Color online) Fourier analysis (DFT) together with 99 % (red) and 95 % (green) confidence lines of the T(t) resp. $P(t)$ time series. Left upper panel: $P(t)$ record of Steinhilber and Beer (2013). Right upper panel: $T(t)$ record of Büntgen et al. (2011). Left lower panel: $T(t)$ record of Christiansen and Ljungqvist (2012). Right lower panel: $T(t)$ record of Cook et al. (2000).





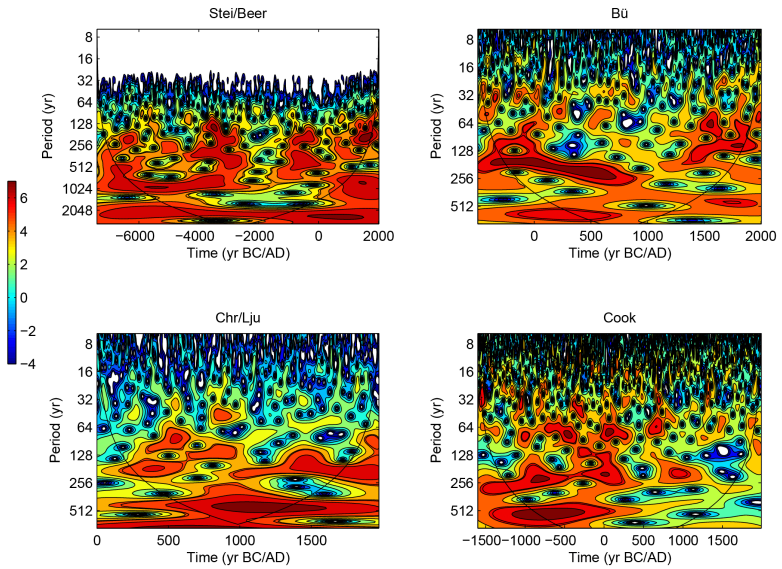


**Figure 4.** (Color online) Wavelet analyses of the $T(t)$ resp. $P(t)$ time series. Left upper panel (Steinhilber and Beer, 2013). Left lower panel (Christiansen and Ljungqvist, 2012). Right upper panel (Büntgen et al., 2011). Right lower panel (Cook et al., 2000).

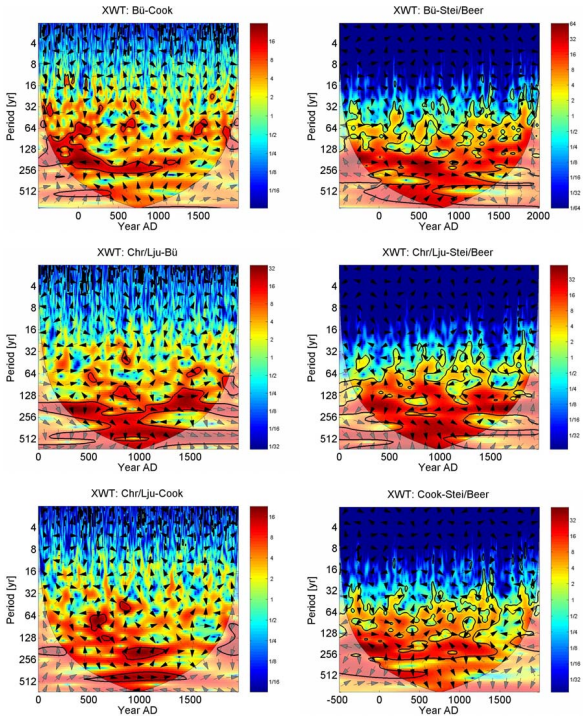


**Figure 5.** (Color online) Cross wavelets of the $T(t)$ resp. $P(t)$ records, results reliable inside the cone of influence. The arrows give the phase relation with in-phase pointing right, anti-phase pointing left and the first record leading the second one by $\pi/2$ pointing straight down (Grinsted et al., 2004).



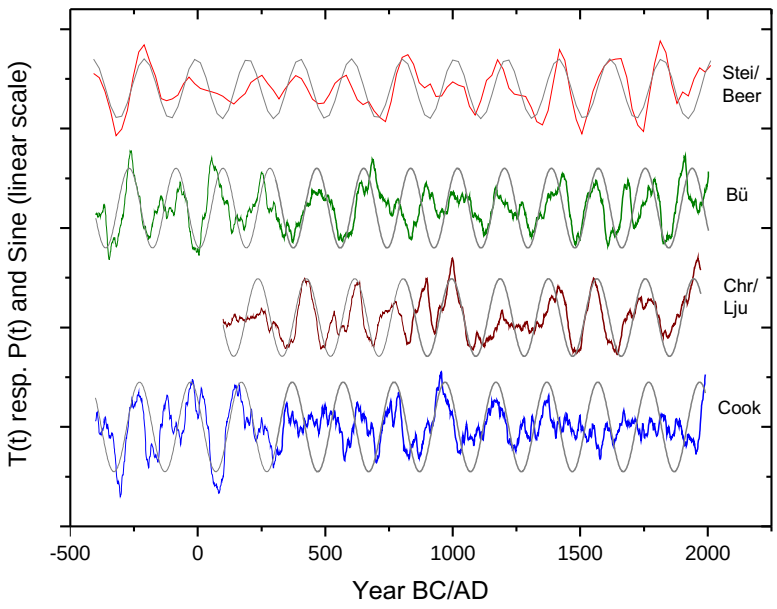


**Figure 6.** (Color online) Representations of the difference records $\Delta T(t)$ resp. $\Delta P(t)$ by a single sine each (grey color) as an outcome of nonlinear optimization, numerical results given in Table 3. The records are normalized to the SD, sine amplitudes arbitrary (not relevant for correlation).

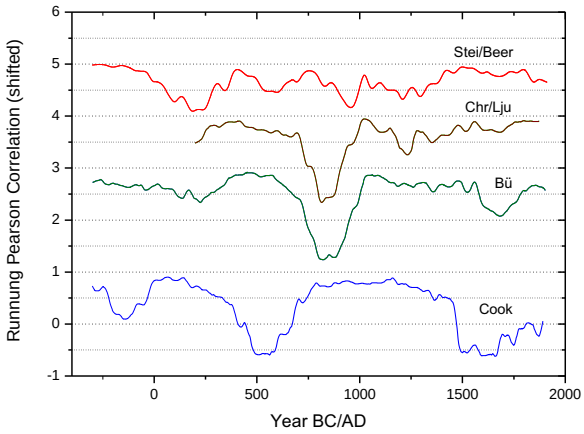


**Figure 7.** (Color online) Running Pearson correlation of $\Delta T(t)$ with $\Delta T_{\text{sine}}$ resp. $\Delta P(t)$ with $\Delta P_{\text{sine}}$, window length 200 years. The curves are shifted for clarity, Bü + 2, Chr/Lju + 3, and Stei/Beer + 4.





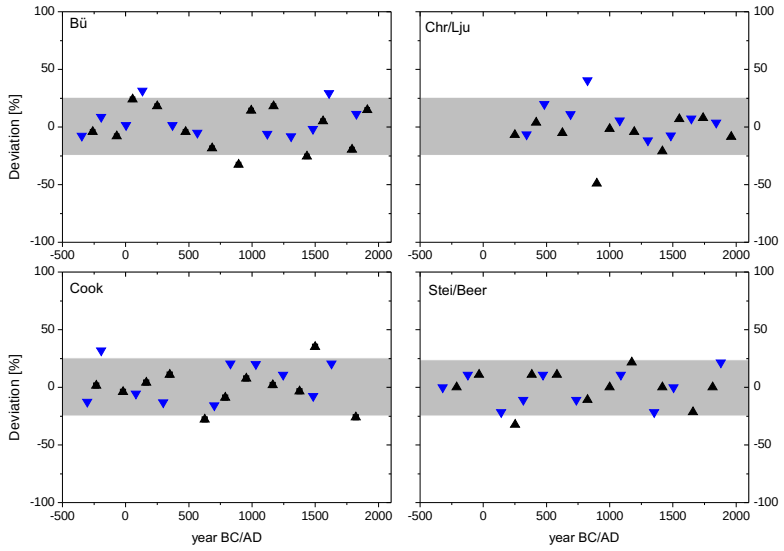


**Figure 8.** (Color online) Deviations of the maxima (black triangles) and minima (blue triangles) from the pertinent sine extrema in % of period length. All records have 1 year time resolution except for Steinhilber/Beer (22 years). Grey shaded areas indicate the ±25 % deviation zone. The minima of the sine representations for Bü at AD 743 and 927, for Cook at AD 470, and for Stei/Beer at AD 912 have no valid analog in the time series (see also Fig. 6).

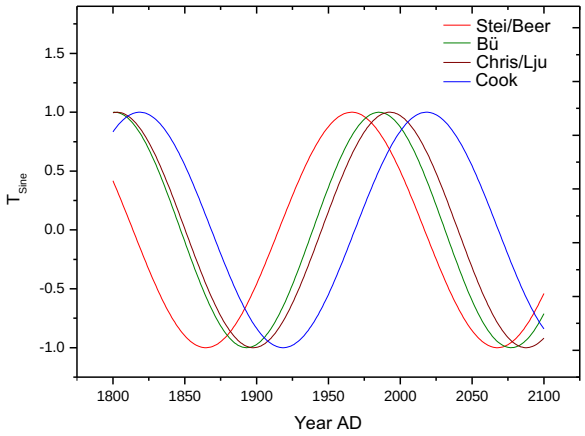


**Figure 9.** (Color online) Sine representations of recent and future climate $T(t)$ according to the $\sim 200$ year period for the data sets of No. 1.0, 2.0, 3.0, and 4.0 of Table 3. Please note that this is the $T_{\text{sine}}$ representation, which differs from the $\Delta T_{\text{sine}}$ representation shown in Fig. 6 only by $\pi/2$ in phase.